

Crystal Structures, Phase-Transition, and Photoluminescence of Rare Earth Carbodiimides

Jochen Glaser,[†] Leonid Unverfehrt,[†] Helga Bettentrup,[‡] Gunter Heymann,[§] Hubert Huppertz,[§] Thomas Jüstel,[‡] and H.-Jürgen Meyer^{*†}

Abteilung für Festkörperchemie und Theoretische Anorganische Chemie, Institut für Anorganische Chemie, Universität Tübingen, Ob dem Himmelreich 7, D-72074 Tübingen, Germany, Fachbereich Chemieingenieurwesen, Fachhochschule Münster, Abteilung Steinfurt, Stegerwaldstrasse 39, D-48565 Steinfurt, Germany, and Institut für Allgemeine, Anorganische und Theoretische Chemie, Leopold-Franzens-Universität, Innsbruck, Innrain 52 a, A-6020 Innsbruck, Austria

Received May 30, 2008

Rare earth carbodiimides with the general formula $\text{RE}_2(\text{CN}_2)_3$ crystallize with two modifications. A monoclinic ($C2/m$) modification is obtained for $\text{RE} = \text{Y}, \text{Ce}–\text{Tm}$ and a rhombohedral ($R\bar{3}c$) modification for $\text{RE} = \text{Tm}–\text{Lu}$. The space group $R\bar{3}c$ is confirmed by single-crystal structure determination on $\text{Lu}_2(\text{CN}_2)_3$ and indexed powder patterns of $\text{RE} = \text{Tm}, \text{Yb}$ and Lu . The use of diverse chemical syntheses conditions for $\text{Tm}_2(\text{CN}_2)_3$ revealed the dimorphic character of this compound. In addition, pressure experiments on $\text{Tm}_2(\text{CN}_2)_3$ have induced a phase-transition from rhombohedral to monoclinic. This transformation comprises an increase of the coordination number of Tm from 6 to 7, and a unit-cell volume reduction in the order of 20 %. The photoluminescence behavior of lanthanide doped $\text{Gd}_2(\text{CN}_2)_3:\text{Ln}$ samples is presented with different activators ($\text{Ln} = \text{Ce}, \text{Tb}$) revealing a broad band emission of $\text{Gd}_2(\text{CN}_2)_3:\text{Ce}$, quite similar to that of the well-known YAG:Ce.

Introduction

Recently, a number of new carbodiimide structures (in some cases also cyanamides) were reported and structurally characterized in the field of transition metal (M) and rare earth metal (RE) chemistry. Transition metal carbodiimides $\text{M}(\text{CN}_2)$ are known with $\text{M} = \text{Mn}, \text{Fe}, \text{Co}, \text{Ni}$, and Cu .¹ Several families of rare earth carbodiimide compounds were described having formulas $\text{RE}_2(\text{CN}_2)_3$,² $\text{RECl}(\text{CN}_2)$,³ $\text{RE}_2\text{Cl}(\text{CN}_2)\text{N}$,⁴ $\text{RE}_2\text{O}(\text{CN}_2)_2$,⁵ $\text{RE}_2\text{O}_2(\text{CN}_2)$,⁶ including some recent examples such as $\text{REF}(\text{CN}_2)$, and $\text{LiRE}_2\text{F}_3(\text{CN}_2)_2$.⁷

Solid state metathesis reactions⁸ launched with gentle heating conditions play a key role in making these compounds because this particularly suitable method allows syntheses even of thermally labile compounds.

Although most of these compounds are moderately stable in air, their potentials or properties are sparsely investigated. Photoluminescence properties were reported for $\text{RE}_2\text{O}_2(\text{CN}_2):\text{Ln}$ compounds,⁹ with $\text{Y}_2\text{O}_2(\text{CN}_2):\text{Eu}$ ¹⁰ having very similar

* To whom correspondence should be addressed. E-mail: juergen.meyer@uni-tuebingen.de. Fax: +49 7071 29 5702 or +49 7071 29 76226.

[†] Institut für Anorganische Chemie, Universität Tübingen.

[‡] Fachbereich Chemieingenieurwesen, Fachhochschule Münster, Steinfurt.

[§] Institut für Allgemeine, Anorganische und Theoretische Chemie, Leopold-Franzens-Universität.

(1) (a) Liu, X.; Krott, M.; Müller, P.; Hu, C.; Lueken, H.; Dronskowski, R. *Inorg. Chem.* **2005**, *44*, 3001–3003. (b) Krott, M.; Liu, X.; Fokwa, B. P. T.; Speldrich, M.; Lueken, H.; Dronskowski, R. *Inorg. Chem.* **2007**, *46*, 2204–2207. (c) Liu, X.; Wankeu, M. A.; Lueken, H.; Dronskowski, R. *Z. Naturforsch.* **2005**, *B60*, 593–596.

(2) Neukirch, M.; Tragl, S.; Meyer, H.-J. *Inorg. Chem.* **2006**, *45*, 8188–8193.

(3) Srinivasan, R.; Glaser, J.; Tragl, S.; Meyer, H.-J. *Z. Anorg. Allg. Chem.* **2005**, *631*, 479–483.

(4) Srinivasan, R.; Ströbele, M.; Meyer, H.-J. *Inorg. Chem.* **2003**, *42*, 3406–3411.

(5) Srinivasan, R.; Tragl, S.; Meyer, H.-J. *Z. Anorg. Allg. Chem.* **2005**, *631*, 719–722.

(6) Hashimoto, Y.; Takahashi, M.; Kikkawa, S.; Kanamaru, F. *J. Solid State Chem.* **1995**, *114*, 592–594; **1996**, *125*, 37–42.

(7) Unverfehrt, L. Diploma Thesis, University of Tübingen, Tübingen, Germany, 2007.

(8) Gibson, K.; Ströbele, M.; Blaschkowski, B.; Glaser, J.; Weisser, M.; Srinivasan, R.; Kolb, H.-J.; Meyer, H.-J. *Z. Anorg. Allg. Chem.* **2003**, *629*, 1863–1870.

(9) Takahashi, M.; Hashimoto, Y.; Kikkawa, S.; Kobayashi, H. *Zairyo* **2000**, *49*, 1230–1234.

(10) Sindlinger, J.; Glaser, J.; Bettentrup, H.; Jüstel, T.; Meyer, H.-J. *Z. Anorg. Allg. Chem.* **2007**, *633*, 1686–1690.

luminescence properties as the well-known red-light emitter $\text{Y}_2\text{O}_2\text{S}:\text{Eu}$.

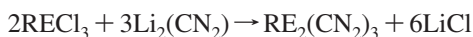
Rare earth carbodiimides with the general formula $\text{RE}_2(\text{CN}_2)_3$ were reported to occur with two different structures. Compounds with larger rare earth elements crystallize monoclinically, and those with smaller (or late) rare earth elements crystallize rhombohedrally.² The occurrence of two or more modifications is not uncommon among the rare earth series, such as for sesquioxides (RE_2O_3) or sesquisulfides (RE_2S_3).¹¹

The only missing or unconfirmed $\text{RE}_2(\text{CN}_2)_3$ compounds were those with $\text{RE} = \text{Sc}, \text{La},^{12} \text{Ce}, \text{Pm},$ and Eu . A europium compound was reported as $\text{Eu}(\text{CN}_2)_2$, containing divalent europium.¹³ Recently, Reckeweg et al. published the crystal structure of $\text{Yb}_2(\text{CN}_2)_3$ solved and refined in the space group $R\bar{3}c$.¹⁴

Within this work, we report the new compound $\text{Ce}_2(\text{CN}_2)_3$, and retract our earlier choice of $R32^2$ confirming the centrosymmetric space group $R\bar{3}c$ for compounds with $\text{RE} = \text{Tm}, \text{Yb},$ and Lu . In addition, we provide a synthesis route for rhombohedral but also for the new monoclinic phase of $\text{Tm}_2(\text{CN}_2)_3$, and an experimental study of a pressure induced phase-transition of $\text{Tm}_2(\text{CN}_2)_3$ from rhombohedral to monoclinic, so as to present the relationship between the two different crystal structures. Finally, the photoluminescence behavior of $\text{Gd}_2(\text{CN}_2)_3:\text{Ln}$ is presented with $\text{Ln} = \text{Ce}, \text{Tb}$ as activators.

Experimental Section

Syntheses. Preparation of starting materials, their handling, manipulations, and the solid state metathesis reactions were performed as previously reported:²



$\text{Li}_2(\text{CN}_2)$ was made by treating $\text{Li}_2(\text{CO}_3)$ (2 g, Alfa, ultrapure) in flowing ammonia at 660 °C (6–8 h) several times, inclusive regrinding, until a single-phase product was obtained.¹⁵ The missing compound $\text{Ce}_2(\text{CN}_2)_3$ was synthesized from CeCl_3 (ABCR, 99.9 %) and $\text{Li}_2(\text{CN}_2)$ in a 2:3 molar ratio (ca. 150 mg), reacted in an evacuated silica ampoule for 3 days at 500 °C. Reactions designed to synthesize $\text{La}_2(\text{CN}_2)_3$ at various temperatures between 450 and 600 °C failed to yield $\text{LaCl}(\text{CN}_2)$.³

Crystalline powders of rhombohedral $\text{Tm}_2(\text{CN}_2)_3$ were obtained from a $\text{TmCl}_3/\text{Li}_2(\text{CN}_2)$ mixture (total mass ca. 400 mg) reacted at 550 °C over 5 days in a tantalum ampoule, fused in silica. The product was used for the multianvil high-pressure experiment after washing away the side phases (see below). Powders of the Yb- and Lu-compounds (Table 1) were prepared as reported previously.²

Crystalline light brownish powders of monoclinic $\text{Tm}_2(\text{CN}_2)_3$ were obtained by reacting a $\text{TmF}_3/\text{Li}_2(\text{CN}_2)$ mixture at temperatures between 500–600 °C over 4 days in evacuated silica ampoules. The employed TmF_3 was synthesized by reacting Tm_2O_3 (Ampere,

Table 1. Lattice Parameters (Å) and Unit-Cell Volumes (Å³) of Rhombohedral ($R\bar{3}c$) $\text{RE}_2(\text{CN}_2)_3$ Compounds Calculated from X-ray Powder Data

compound	<i>a</i>	<i>c</i>	<i>V</i>	no. of used reflections
$\text{Tm}_2(\text{CN}_2)_3$	6.3434(2)	29.5486(8)	1029.69(6)	61
$\text{Yb}_2(\text{CN}_2)_3$	6.295(1)	29.448(5)	1010.6(4)	24
$\text{Lu}_2(\text{CN}_2)_3$	6.2805(2)	29.4532(9)	1006.11(6)	70

99.9 %) with NH_4F (1:10 molar ratio) at 100 °C in a corundum beaker in air. The excess of NH_4F was sublimed off and the resulting $(\text{NH}_4)_2\text{TmF}_6$ was decomposed to obtain pure TmF_3 at 380 °C under vacuum.¹⁶ Doped compounds for luminescence studies having the formula type $\text{Gd}_2(\text{CN}_2)_3:\text{Ln}$ were synthesized with $\text{Ln} = \text{Ce}$ and Tb as activators. The amount of GdCl_3 in the starting mixture was lowered in favor of varying amounts of LnCl_3 , allowing contents of 1–10 mol % Ln to be incorporated into the structures $\text{Gd}_{2-x}\text{Ln}_x(\text{CN}_2)_3$. These light grayish powders were prepared in lower temperature regimes (e.g. 500 °C) and with shorter reaction durations (e.g. 2 days). At higher reaction temperatures or longer reaction durations brown to black powders were obtained, probably because of partial decomposition. However, the XRD patterns of the products did not indicate any phases other than $\text{Gd}_{2-x}\text{Ln}_x(\text{CN}_2)_2$.

Single-crystals of $\text{Lu}_2(\text{CN}_2)_3$ were obtained from a $\text{LuCl}_3/\text{Li}_2(\text{CN}_2)$ mixture reacted for 3 weeks in a silica fused tantalum ampoule at 650 °C, using an eutectic (approximately 59 %/41 %) LiCl/KCl flux.

All products were washed with water to remove the coproduced LiCl and rinsed with acetone or ethanol right afterwards. Products can be usually obtained as single-phases, according to X-ray powder diffraction. $\text{RE}_2(\text{CN}_2)_3$ compounds remain stable in air, but slow decomposition into carbonates is obtained by infrared spectroscopy when they are stored in water.

X-ray Powder Diffraction. Diffraction data were collected on a Stoe StadiP X-ray powder diffractometer using Ge-monochromatized $\text{Cu}-\text{K}\alpha_1$ radiation. The powder pattern of the new $\text{Ce}_2(\text{CN}_2)_3$ was indexed monoclinically (from 45 reflections) yielding lattice parameters of $a = 14.968(5)$ Å, $b = 4.028(1)$ Å, $c = 5.337(1)$ Å, and $\beta = 96.19(1)^\circ$.

Reactions designed to synthesize $\text{Tm}_2(\text{CN}_2)_3$ via the new fluoride metathesis reaction yielded powders of monoclinic $\text{Tm}_2(\text{CN}_2)_3$, containing LiF and some LiTmF_4 ¹⁷ as byproducts. An indexed powder pattern yielded lattice parameters of $a = 14.084(3)$ Å, $b = 3.7210(7)$ Å, $c = 5.1812(9)$ Å, and $\beta = 95.49(1)^\circ$ for monoclinic $\text{Tm}_2(\text{CN}_2)_3$, based on 33 indexed X-ray reflections.

Powder patterns of $\text{RE}_2(\text{CN}_2)_3$ with $\text{RE} = \text{Tm}, \text{Yb}, \text{Lu}$ were revisited. Reflections were indexed rhombohedrally resulting in lattice parameters with doubled *c*-axes with respect to our previous report² (Table 1) and, thus, consistent with the centrosymmetric space group $R\bar{3}c$.

Rhombohedral $\text{Tm}_2(\text{CN}_2)_3$ synthesized by the chloride metathesis reaction, with lattice parameters given in Table 1, was used in a high-pressure experiment. The X-ray pattern collected from the $\text{Tm}_2(\text{CN}_2)_3$ sample after the high-pressure treatment was indexed at ambient pressure with a C-centered monoclinic crystal system, yielding lattice parameters of $a = 14.110(2)$ Å, $b = 3.725(1)$ Å, $c = 5.203(9)$ Å, and $\beta = 95.68(9)^\circ$. Deviations of the lattice parameters from (monoclinic) $\text{Tm}_2(\text{CN}_2)_3$ synthesized by the fluoride metathesis may be due to the lower quality of the powder pattern recorded from the product after the high-pressure experiment. The pressure transformation from rhombohedral $\text{Tm}_2(\text{CN}_2)_3$ into monoclinic $\text{Tm}_2(\text{CN}_2)_3$ involves a volume reduction in the order of 20 % from $V/Z = 171.62(6)$ Å³ to $135.1(1)$ Å³.

(11) Zinkevich, M. *Prog. Mater. Sci.* **2007**, *52*, 597–647.

(12) Hartmann, H.; Eckelmann, W. *Z. Anorg. Allg. Chem.* **1948**, *257*, 183–194.

(13) Reckeweg, O.; DiSalvo, F. J. *Z. Anorg. Allg. Chem.* **2003**, *629*, 177–179.

(14) Reckeweg, O.; Schleid, T.; DiSalvo, F. J. *Z. Naturforsch.* **2007**, *62b*, 658–662.

(15) Perret, A. *Bl. Soc. Ind. Mulhouse* **1933**, *99*, 10–20.

(16) Keller, C.; Schumtz, H. *J. Inorg. Nucl. Chem.* **1965**, *27*, 900–901.

(17) Rajeshwar, K.; Secco, E. A. *Can. J. Chem.* **1977**, *55*, 2620–2627.

Table 2. Crystallographic Data for $\text{Lu}_2(\text{CN}_2)_3$

chemical formula	$\text{Lu}_2(\text{CN}_2)_3$
a	6.267(1) Å
c	29.367(6) Å
V	998.8(3) Å ³
Z	6
formula weight	470.03
space group	$R\bar{3}c$ (No. 165)
T	293 K
λ	0.71073 Å
d_{calc}	4.69 g cm ⁻³
μ	294.06 cm ⁻¹
R_1, wR_2 (all data)	0.0246, 0.0307

Table 3. Selected Interatomic Distances (Å) and the N–C–N Angle (deg) for $\text{Lu}_2(\text{CN}_2)_3$

Lu–N	2.279(4)	3 ×
Lu–N	2.330(3)	3 ×
N–C	1.211(3)	2 ×
N–C–N	179.9(7)	

X-ray Single-Crystal Diffraction. Transparent single-crystals of $\text{Lu}_2(\text{CN}_2)_3$ were selected and fixed on the tip of a glass fiber for a single-crystal diffraction measurement (Stoe IPDS diffractometer, graphite monochromatized Mo– K_α radiation) at room temperature (Table 2). Intensities were corrected for Lorentz factors, polarization, and absorption effects. $\text{Lu}_2(\text{CN}_2)_3$ was found to crystallize rhombohedrally with the space group $R\bar{3}c$. Structure refinement and anisotropic refinements with the program SHELX¹⁸ resulted in $R_1 = 0.0246$ and $wR_2 = 0.0307$ for all 4918 measured X-ray intensities. Crystallographic data are given in Table 2 and interatomic distances are provided in Table 3.

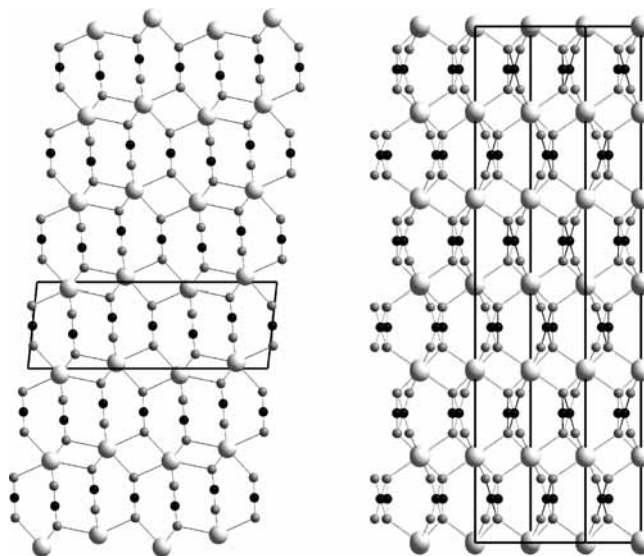
Infrared Spectroscopy. A sample of rhombohedral $\text{Tm}_2(\text{CN}_2)_3$ was mixed with KBr and pressed into a pellet ($\varnothing = 1.3$ cm). The infrared measurement was performed with a Perkin Elmer FT-IR spectrometer within the range of 4000–400 cm⁻¹. The spectrum was corrected for the presence of KBr. The spectral resolution was 2 cm⁻¹. The obtained spectrum displayed the non-symmetric stretch (ν_{as}) of $[\text{NCN}]^{2-}$ at 2070 and 2000 cm⁻¹ and the deformation vibrations at 678 and 640 cm⁻¹.

High-Pressure Phase-Transformation. The high-pressure/high-temperature treatment took place via a multianvil assembly. Details concerning the construction of the assembly can be found in references.^{19–22} A boron nitride crucible of an 18/11-assembly was loaded with carefully milled rhombohedral $\text{Tm}_2(\text{CN}_2)_3$, compressed within 3 h to 7.5 GPa and heated to 650 °C for the following 10 min. After holding this temperature for 10 min, the sample was cooled down to room temperature within 10 minutes. After a decompression period of 9 h, the sample was carefully separated from the surrounding assembly parts.

Photoluminescence Studies. A fluorescence spectrometer (Edinburgh Instrument, FS920, equipped with a 450 W Xe-lamp) was used for the measurement of excitation and emission spectra, all monitored by a cooled photomultiplier tube (Hamamatsu R2658, detection range: 300–1010 nm) driven in a single photon counting mode.

Results and Discussion

Syntheses of $\text{RE}_2(\text{CN}_2)_3$ compounds were accomplished by solid state metathesis reactions of $\text{Li}_2(\text{CN}_2)$ with RECl_3

**Figure 1.** Projection of layered monoclinic (left) and trigonal (right) $\text{RE}_2(\text{CN}_2)_3$ structures along their stacking directions.

or REF_3 , respectively. Exothermic reactions are obtained above 400 °C, sometimes near 500 °C, depending on the individual RECl_3 compound, as monitored by thermo-analytic studies. The employment of an eutectic LiCl/KCl flux (melting point: 354.4 °C) has been advantageous especially for single-crystal growth. The new compound $\text{Ce}_2(\text{CN}_2)_3$ was successfully synthesized at temperatures near 500 °C, whereas the synthesis of $\text{La}_2(\text{CN}_2)_3$ ¹² has still not been confirmed, obviously because of the competing stability of $\text{LaCl}(\text{CN}_2)$ in this temperature regime.

$\text{RE}_2(\text{CN}_2)_3$ compounds remain quite stable in air for days or weeks. Slow decomposition in the presence of moist air or water can be monitored by infrared spectroscopy, rather than by X-ray diffraction, through the appearance of weak bands that can be assigned with those of carbonate ions. This rather slow decomposition process, that obviously begins on the surface of the crystalline material, can be viewed as an inverse process to the synthesis of carbodiimides from carbonates and ammonia.¹⁵ The infrared spectrum of rhombohedral $\text{Tm}_2(\text{CN}_2)_3$ showed characteristic bands of $[\text{N}=\text{C}=\text{N}]^{2-}$ ions^{2,12} and the absence of carbonate.

A reinvestigation of the rhombohedral crystal structure, inspired by results of the study on $\text{Lu}_2(\text{CN}_2)_3$,¹⁴ confirmed the centrosymmetric space group $R\bar{3}c$ also for $\text{Yb}_2(\text{CN}_2)_3$, being closely related to the structure of $\text{In}_{2.24}(\text{CN}_2)_3$.²³ This was also approved for $\text{RE}_2(\text{CN}_2)_3$ compounds with $\text{RE} = \text{Tm}, \text{Yb}, \text{Lu}$ from indexed powder patterns (Table 1).

After the rhombohedral modification of $\text{Tm}_2(\text{CN}_2)_3$ has been already known, a monoclinic modification of $\text{Tm}_2(\text{CN}_2)_3$ was established via two independent ways: (a) by fluoride metathesis reaction and (b) by high-pressure transformation of rhombohedral $\text{Tm}_2(\text{CN}_2)_3$.

Thus, $\text{RE}_2(\text{CN}_2)_3$ compounds crystallize monoclinically ($C2/m$) for $\text{RE} = \text{Y}, \text{Ce}–\text{Tm}$ (except Pm and Eu) and rhombohedrally ($R\bar{3}c$) for $\text{RE} = \text{Tm}, \text{Yb}, \text{Lu}$ (Figures 1 and 2). Among these, $\text{Tm}_2(\text{CN}_2)_3$ occurs dimorphic with both

(18) Sheldrick, G. M. *Acta Crystallogr., Sect. A: Found. Crystallogr.* **2008**, *64*, 112–122.

(19) Huppertz, H. Z. *Kristallogr.* **2004**, *219*, 330–338.

(20) Walker, D.; Carpenter, M. A.; Hitch, C. M. *Am. Mineral.* **1990**, *75*, 1020–1028.

(21) Walker, D. *Am. Mineral.* **1991**, *76*, 1092–1100.

(22) Rubie, D. C. *Phase Transitions* **1999**, *68*, 431–451.

(23) Dronskowski, R. *Z. Naturforsch.* **1995**, *50b*, 1245–1251.

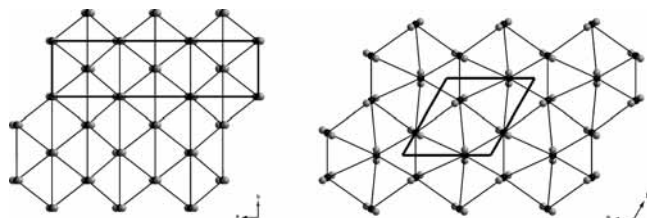


Figure 2. Single layers of [NCN] anions adopted from monoclinic (left) and trigonal (right) $\text{RE}_2(\text{CN}_2)_3$ structures.

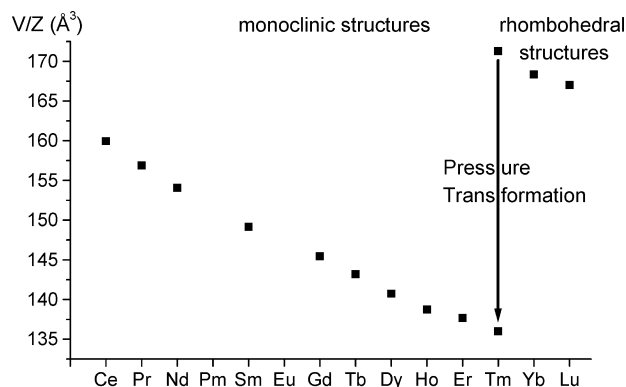


Figure 3. Dependency of the unit cell volume per formula unit (V/Z) versus relative radii of rare earth ions of monoclinic and rhombohedral $\text{RE}_2(\text{CN}_2)_3$ structures, including dimorphic $\text{Tm}_2(\text{CN}_2)_3$.

structure types, and europium carbodiimide is known as $\text{Eu}(\text{CN}_2)$ containing Eu^{2+} .¹³

The lanthanide contraction within this series of compounds involves one major jump (Figure 3), as a consequence of the intrinsic larger volume per formula unit (V/Z) of the rhombohedral structures with $\text{RE} = \text{Tm}, \text{Yb}, \text{Lu}$. A comparison of monoclinic and rhombohedral $\text{RE}_2(\text{CN}_2)_3$ structures is displayed in Figures 1 and 2. Both structures contain layers of RE atoms alternating with layers of [NCN] sticks. Differences between both structures can be expressed as follows: Monoclinic $\text{RE}_2(\text{CN}_2)_3$ structures contain wavy layers of larger RE cations and layers of parallel aligned [NCN] anions. Rhombohedral $\text{RE}_2(\text{CN}_2)_3$ structures contain planar layers of smaller RE cations and layers of tilted [NCN] anion arrangements. The displacement of the RE cations from the center of a distorted monocapped trigonal-prismatic environment of N-atoms in monoclinic structures allows for seven next N-neighbors of [NCN] units, whereas the position of smaller cations on the three-fold axis of rhombohedral structures is close to an octahedral environment (Figure 4), similar as for aluminum ions in the corundum structure. The array of tilted [NCN] sticks in rhombohedral structures induces a much higher volume increment because the parallel [NCN] sticks in monoclinic structures resemble more alike the principle of a hexagonal closest stick packing (Figure 2).

A pressure experiment performed on rhombohedral $\text{Tm}_2(\text{CN}_2)_3$ revealed a transformation into the monoclinic structure, accompanied with a significant volume shrinkage in the order of 20%. The obtained cell volume of monoclinic $\text{Tm}_2(\text{CN}_2)_3$ nicely complements the trend within the series of monoclinic structures, as shown in Figure 3.

The occurrence of two or more different structures is not uncommon along the series of homologous rare earth

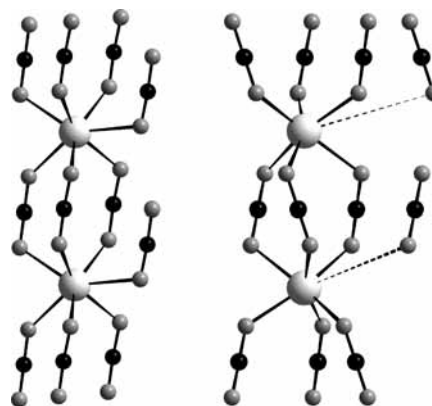


Figure 4. Comparison of the environment of RE ions with carbodiimide ions in monoclinic (left) and rhombohedral (right) $\text{RE}_2(\text{CN}_2)_3$. One out of three equivalent [NCN] units in the further distant vicinity ($> 4.5 \text{ \AA}$) of each RE are shown in rhombohedral $\text{RE}_2(\text{CN}_2)_3$ (connected with a dashed line) to emphasize the relationship between both structures.

compounds and can be often explained as a result of the contraction of ionic radii (lanthanide contraction). Generally, the contraction of the RE^{3+} radii along a series of homologous compounds involves growing anion-anion repulsions until another structure type can appear. The change of $\text{RE}_2(\text{CN}_2)_3$ structures could be explained as the result of an increased tilting of carbodiimide groups, with a huge expansion within layers in the structures.

Rare earth oxychlorides with the general formula REOCl are reported to crystallize in the PbFCl type structure for $\text{RE} = \text{La}-\text{Er}$, and in the SmSI type for $\text{RE} = \text{Er}-\text{Lu}$, with ErOCl being dimorphic. High-pressure phase-transformations involve conversions of the latter group of compounds from the SmSI into the PbFCl type structure.²⁴ High-pressure transitions of ErOCl afford volume shrinkages of about 13%.

To study the potential of the novel $\text{RE}_2(\text{CN}_2)_3$ compounds as luminescent materials for fluorescent light sources or emissive displays, $\text{Gd}_2(\text{CN}_2)_3$ was doped by either Ce^{3+} , Tb^{3+} , or Ce^{3+} and Tb^{3+} .

The luminescence spectra of the Ce^{3+} doped materials are governed by an interconfigurational transition between the ground state levels ($^2F_{5/2}$ and $^2F_{7/2}$) of the $[\text{Xe}]4f^1$ configuration and the lowest crystal-field components of the $[\text{Xe}]5d^1$ configuration. This is a spin and parity allowed transition, resulting in high oscillator strength and a short decay constant.²⁴

Because of the involvement of d orbitals in chemical bonding, the energy of the crystal-field components of the $[\text{Xe}]5d^1$ configuration is a sensitive function of the chemical environment. Ce^{3+} activated luminescent materials can thus show UV, blue, green, or red luminescence, whereby the energetic position of the absorption and emission bands are determined by the crystal-field strength and the covalent character of the lattice position, where Ce^{3+} is localized.

Enhancing the crystal-field strength and/or the covalent interaction between the activator and the surrounding ligands yields a reduction of the energy gap between the excited state and ground state configuration. Ligands with a high

(24) Beck, H. P. Z. *Naturforsch.* **1976**, *31b*, 1562–1564; **1977**, *32b*, 1015–1021.

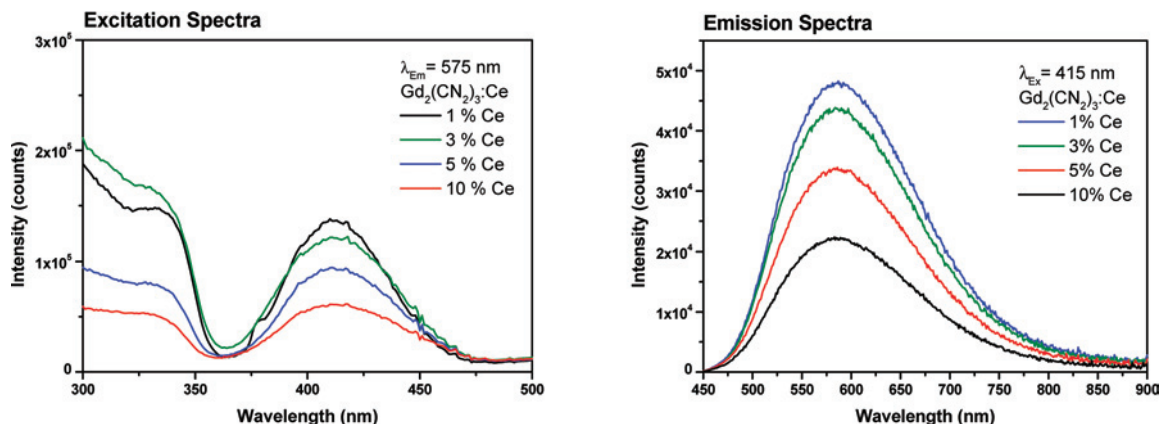


Figure 5. Excitation and emission spectra of $\text{Gd}_2(\text{CN}_2)_3:\text{Ce}^{3+}$ for several Ce^{3+} concentrations. Emission spectra were taken under 415 nm excitation, and excitation spectra were monitored for 575 nm emission.

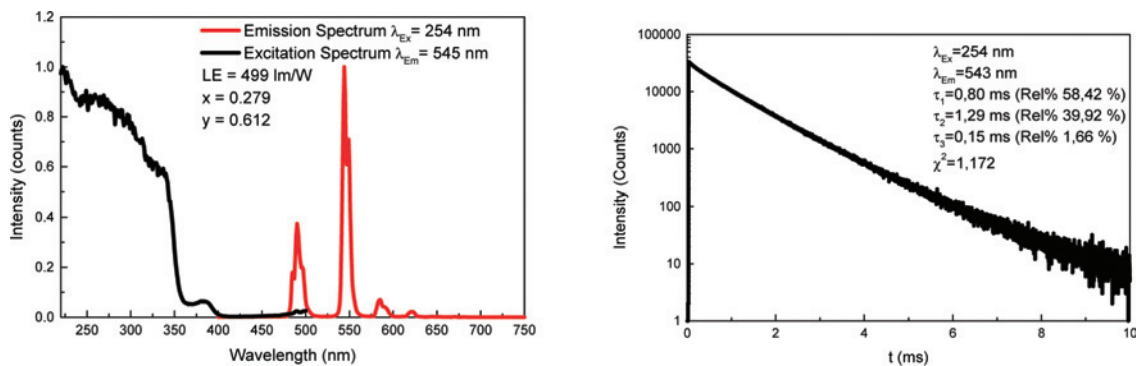


Figure 6. Excitation spectrum, emission spectrum, and decay curve of $\text{Gd}_2(\text{CN}_2)_3:\text{Tb}^{3+}$. The excitation spectrum was monitored for 545 nm emission. The emission spectrum and the decay curve were recorded under 254 nm excitation.

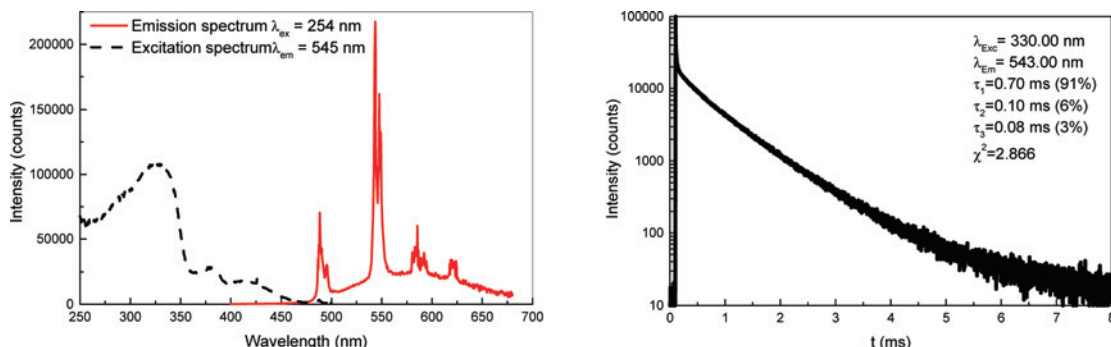


Figure 7. Excitation spectrum, emission spectrum and decay curve of $\text{Gd}_2(\text{CN}_2)_3:\text{Ce}^{3+}\text{Tb}^{3+}$. The excitation spectrum was monitored for 545 nm emission. The emission spectrum and the decay curve were recorded under 254 nm excitation.

negative charge density (alkalinity) show a strong covalent interaction with the metal cations, that is, with the activator.

The maximum of the emission band of $\text{Gd}_2(\text{CN}_2)_3:\text{Ce}$ is at approximately 575 nm (Figure 5), which is compared to the widely applied light-emitting diode (LED) phosphor $\text{Y}_3\text{Al}_5\text{O}_{12}:\text{Ce}^{3+}$ (YAG:Ce),²⁵ a distinct red shift of about 15 nm. However, the maximum of the lowest excitation band is located at 415 nm, and thus 35 nm blue-shifted compared to YAG:Ce. This means that the Stokes Shift is distinctly larger, which can be explained by a stronger electron-phonon coupling in carbodiimide hosts compared to oxide hosts.

The CIE 1931 color point of $\text{Gd}_2(\text{CN}_2)_3:\text{Ce}^{3+}$ is at $x = 0.505$ and $y = 0.480$, that is, the material is an amber emitting

luminescent material, and indeed red-shifted compared to YAG:Ce ($x = 0.459$ and $y = 0.527$). The emission peak position and color point hardly shifts with the Ce^{3+} concentration, which proves the lack of efficient re-absorption. This was expected from the fluorescence spectra, since the broad excitation and emission band show little spectral overlap.

Doping of $\text{Gd}_2(\text{CN}_2)_3$ by Tb^{3+} results in an efficient luminescent material with a decay time of about 1 ms and the typical emission peak pattern of Tb^{3+} activated host lattices (Figure 6), while the peak multiplets at 490, 543, 590, and 620 nm can be assigned to the $^5\text{D}_4 \rightarrow ^7\text{F}_j$ ($J = 3-6$) transitions.²⁶ The CIE 1931 color point of $\text{Gd}_2(\text{CN}_2)_3:\text{Tb}^{3+}$ is at $x = 0.279$ and $y = 0.612$, that is, the material is a green emitting luminescent material. It should be noted

(25) Blasse, G.; Grabmaier, B. C. *Luminescent Materials*; Springer Verlag: New York, 1994; Chapter 3.3, p 45.

(26) Born, M.; Jüstel, T. *Chemie in unserer Zeit* **2006**, *40*, 294–305.

that the y -value of this $\text{Gd}_2(\text{CN}_2)_3:\text{Tb}^{3+}$ is higher than that of many other Tb^{3+} activated materials, for example, $\text{LaPO}_4:\text{Ce,Tb}$, $\text{GdMgB}_5\text{O}_{10}:\text{Ce,Tb}$, or $\text{Tb}[\text{N}(\text{CN})_2]_3$ ($x = 0.334$, $y = 0.568$).²⁷ This is caused by the high intensity of the $^5\text{D}_4 \rightarrow ^7\text{F}_5$ transition at 543 nm relative to the $^5\text{D}_4 \rightarrow ^7\text{F}_4$ (590 nm) and $^5\text{D}_4 \rightarrow ^7\text{F}_3$ (620 nm) transitions. The excitation spectrum of $\text{Gd}_2(\text{CN}_2)_3:\text{Tb}^{3+}$ exhibits a weak and narrow band at 380 nm, which can be attributed to the $^7\text{F}_J - ^5\text{D}_3$ transitions of Tb^{3+} and several intense and overlapping bands between 220 and 350 nm, which are assigned as 4f^8 to $4\text{f}^75\text{d}^1$ transitions of Tb^{3+} . It should be noted that the energy of these 4f^8 to $4\text{f}^75\text{d}^1$ transitions is rather low, which is in contradiction to Tb^{3+} phosphors based on oxides or fluorides,^{27,28} but in line with the results on $\text{Tb}[\text{N}(\text{CN})_2]_3$.²⁹

An excitation of $\text{Gd}_2(\text{CN}_2)_3$ doped with Tb^{3+} and Ce^{3+} at 254 nm yields an emission spectrum with the broad emission band of Ce^{3+} superimposed by emission lines due to the $^5\text{D}_4 \rightarrow ^7\text{F}_J$ ($J = 3-6$) transitions of Tb^{3+} (Figure 7). Monitoring the excitation spectrum for the $^5\text{D}_4 \rightarrow ^7\text{F}_5$ transition of Tb^{3+}

at 543 nm results in three bands located at 415 nm ($4\text{f}^1 - 5\text{d}^1$ of Ce^{3+}), 380 nm ($^7\text{F}_J - ^5\text{D}_3$ of Tb^{3+}), and at 330 nm ($4\text{f}^1 - 5\text{d}^1$ of Ce^{3+} and $^7\text{F}_J - ^5\text{D}_3$ of Tb^{3+}). The presence of the band at 415 nm clearly shows that energy transfer from the lowest crystal field component of the excited state of Ce^{3+} to the $^5\text{D}_4$ level of Tb^{3+} takes place. This finding shows that the sensitization of Tb^{3+} is not only possible in the UV range, as exploited in the commercial phosphors $\text{LaPO}_4:\text{Ce,Tb}$ and $\text{GdMgB}_5\text{O}_{10}:\text{Ce,Tb}$, but also in the blue range, which might be of interest for near UV and blue LEDs. The decay curve upon 330 nm excitation monitored for the Tb^{3+} emission at 543 nm confirms this statement, since it shows a steep initial drop, which is not present in the decay curve of $\text{Gd}_2(\text{CN}_2)_3$ solely doped by Tb^{3+} (Figure 6).

Acknowledgment. The authors from Tübingen gratefully acknowledge the support of this research by the Deutsche Forschungsgemeinschaft (Bonn) within the framework of our research project “Nitridocarbonate”.

Supporting Information Available: Additional tables and crystallographic data in CIF format. This material is available free of charge via the Internet at <http://pubs.acs.org>.

IC800985K

(27) Nag, A.; Schmidt, P. J.; Schnick, W. *Chem. Mater.* **2006**, *18*, 5738–5745.

(28) Ning, L.; Mak, C. S. K.; Tanner, P. A. *Phys. Rev. B* **2005**, *72*, 085127.

(29) van Pieterse, L.; Reid, M. F.; Burdick, G. W.; Meijerink, A. *Phys. Rev. B* **2002**, *65*, 045114.